Wavelength-dependent channel power transient response in broadband Raman-amplified transmission

D. C. Kilper,[1,*] A. R. Grant,[2] T. K. Ho,[3] T. Salamon,[3] and C. A. White[3]

[1]*Bell Laboratories, Alcatel-Lucent S. A., 791 Holmdel-Keyport Road, Holmdel, New Jersey 07733, USA*
[2]*LGS Innovations, PO Box 898, Room 1B-413C, 600 Mountain Avenue, Murray Hill, New Jersey, 07974-0898, USA*
[3]*Bell Laboratories, Alcatel-Lucent S. A., 600 Mountain Avenue, Murray Hill, New Jersey 07974, USA*
**Corresponding author: dkilper@alcatel-lucent.com*

Received August 20, 2007; revised October 27, 2007; accepted October 29, 2007; published January 10, 2008 (Doc. ID 86537)

The time evolution of uncontrolled amplifier gain transients due to dropped or cut dense-wavelength-division multiplexed channels in a broadband all-Raman amplified recirculating loop experiment is measured for different surviving channel wavelength configurations with propagation up to 7200 km. Different time signatures develop depending on whether the surviving channels are located at the long- or short-wavelength end of the spectrum. Channel power tilt and gain error within a surviving channel group can vary with distance and are shown to correlate with growth of amplified spontaneous emission noise at the dropped channel wavelengths. © 2008 Optical Society of America

OCIS codes: 060.0060, 060.2320.

1. Introduction

Broadband Raman amplification has been a cornerstone of record transmission distances in high-capacity dense-wavelength-division multiplexed (DWDM) system experiments [1]. Transparent networking elements such as optical add–drop multiplexers and cross-connects can be used with ultralong reach systems to build optically transparent mesh networks. However, rapid changes in the DWDM channel population due to fiber cuts or component failures can lead to transient power excursions on downstream channels added at these transparent network elements. This behavior was first studied in heavily saturated erbium-doped fiber amplifiers (EDFAs) [2] and shown to require mitigation techniques such as fast pump control [3] or all-optical methods [4]. The transient properties of Raman amplifiers have been the subject of recent studies. For Raman amplification, the gain saturation is much less and the response time is primarily dictated by the intrinsic relaxation times of the amplifier [5–8]. The uncontrolled transient response of cascaded EDFAs is known to exhibit an overshoot that sharpens with the number of amplifiers and places requirements on the control response time for all-EDFA long haul or mesh networks [2]. Overshoots have been observed in single amplifier Raman experiments [5,6] due to excess pump depletion on the transition edge [9]. In all-Raman amplified transmission experiments, the transient event time response for surviving channels on the short-wavelength end of the spectrum was shown to evolve with distance and correlate with the growth of amplified spontaneous emission (ASE) noise power at the cut channel wavelengths [10]. Here we examine the evolution of transient channel power excursions for a broadband all-Raman amplified system as a function of the wavelength of the surviving channels and study the correlation with ASE noise power growth in more detail.

2. Experimental Setup

Long distance, uncontrolled channel power transient propagation is studied using a recirculating loop setup. Six 100 km nonzero dispersion-shifted True-Wave Reduced

 © 2008 Optical Society of America

Slope fiber spans in the recirculating loop (Fig. 1) are backward and forward pumped for a −2 dB net gain that is equally derived from pumping in each direction (10.5 dB ON–OFF Raman gain). The amplifiers used here are identical to those used in [1], with the exception that the dispersion compensation is entirely implemented using dispersion compensating fiber (DCF). The DCF spools are backward pumped to bring the launch power to −9 dBm per channel from 1542 to 1594 nm (9 dB ON–OFF Raman gain). Additional discrete Raman amplifiers (B1–B3) composed of standard single-mode fiber and Raman specialty fiber are used with the dynamic gain-equalizing filter (DGEF) and in the load path (LB). Four unique wavelengths (1425, 1436, 1460, and 1486 nm) are used for the span forward and backward pumps, and three wavelengths (1437, 1462, and 1487 nm) for the DCF amplifiers. The LB loading amplifier uses the same pump wavelengths as the spans amplifiers. The three discrete Raman amplifiers in the loop use 1487, 1462, and 1437 nm for B1; 1425, 1440, 1465, and 1485 nm for B2; and 1426, 1436, 1461, and 1486 nm for B3. In all cases the shortest-wavelength pump was operated with the highest power into the fiber (in some cases approaching a factor of 2 higher than the other pumps) and the 1460 nm pumps with the lowest power—the exact values varied from run to run as required to level the channels. Amplifiers B2 and B3 were composed of specialty Raman gain fiber (8 km) and amplifier B1 was composed of standard single-mode fiber (16 km) in order to compensate for the negative dispersion in B2 and B3. The multimode Raman pumps were polarization scrambled using a short length of birefringent fiber. Ninety-three polarization interleaved channels pass through acousto-optic switches S1 and S2 so that they can be switched off for 1 ms intervals, synchronously with the recirculating loop switches, centered within the 3.3 ms round-trip time. The remaining 16 channels are separately multiplexed and combined with the other channels after the switches, acting as add channels. These 16 surviving channels are chosen in bands either at the long or short end or midpoint of the spectrum. The peak-to-peak ripple of the channel spectra at the input to the loading amplifier was typically less than 2 dB, and after transmission through the six spans this increased to 4–5 dB, which was releveled by the DGEF. After 12 round trips the residual ripple that could not be compensated by the DGEF was 7–9 dB peak-to-peak, although typically less than 5 dB within the region of the surviving channels.

3. Wavelength-Dependent Time Evolution

The time evolution of the channel power excursions resulting from opening switches S1 and S2 were measured at the input to each span at tap M2 for 12 round trips (7200 km). The results for the input to spans 1–6 (nominally 0–500 km), 12 (1100 km), and 72 (7100 km) are shown in Fig. 2, offset vertically in order to align the after transient steady-state powers. Curves are shown for the shortest wavelength channel in the short-wavelength set (blue) and the longest-wavelength channel after the system was reconfigured for the long-wavelength survivor set (red), selected by moving the optical tunable filter (OTF) to tap M2. The mid-wavelength survivor responses fall between these two extreme cases and are not shown for clarity. The traces were collected using a 2 MHz p-i-n photodiode and a high-speed digitizing oscil-

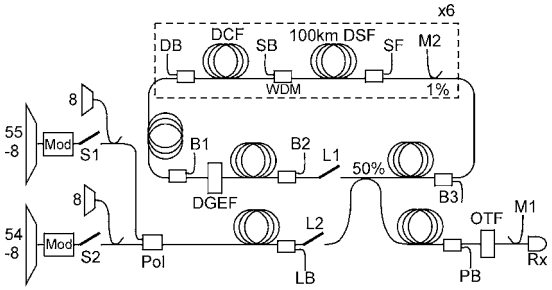


Fig. 1. Six span recirculating loop configuration; M1, M2: monitor points; Mod: 10 Gbits/s RZ pulse carver and data modulator; Pol: polarization combiner; L1, L2: loop closing and loading switches; DGEF: dynamic gain equalizing filter; B1–B3: DGEF amplifier backward pumps; SF: span forward pumps; SB: span backward pumps; DB: DCF backward pumps; LB: load amplifier backward pumps; PB: postcompensating fiber backward pumps; OTF: optical tunable filter; Rx: receiver optoelectronics.

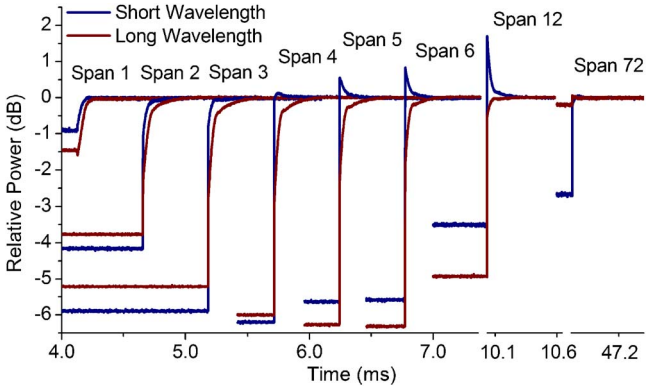


Fig. 2. Time evolution of short- and long-wavelength surviving channels at the input to spans 1–6, 12, and 72 normalized to the final steady-state power. The signature depends on the wavelength of the surviving channel set.

loscope. All of the channels in a given surviving channel set demonstrated qualitatively similar behavior. Note that the span 1 input is the response of the loading Raman amplifier (LB).

The transient response curves in Fig. 2 exhibit time dependent features that act on three different time scales [6]. The copropagating Raman interactions, which include both channel–channel and copropagating pump–channel gain, are dictated by the dispersion walk-off (10–50 ns), which is faster than the switching time (~1 μs) and therefore instantaneous on the scale in Fig. 2. The counterpropagating Raman pump response time is equal to twice the propagation time through the effective length of the amplifier. For the distributed amplification in the spans (L_{eff}~20 km) this of the order of 100–300 ms, and the counterpropagating Raman pumping in the DCF and other discrete amplifiers (L_{eff}~5 km) is in the range of 10–90 ms. By fitting two exponential functions to several of the curves in Fig. 2, we obtain a span 1/e time constant that varies between 190 and 170 μs for the long and short wavelength survivors, respectively, and in the DCF between 30 and 20 μs, respectively. These values are similar to or slightly less than twice the propagation time through the effective length of the amplifiers. Pump depletion due to the channels loading the amplifiers is expected to accelerate the response and could account for these values [9]. The fit to the long-wavelength survivors at the input to span 2 is shown in Fig. 3. Uncertainty in the fit parameters and the formation of features that were not exponential does not allow one to detect a trend in the evolution of the time constants with distance. Nevertheless, the general behavior was consistent among the different curves and the variation with wavelength is expected due to the longer effective length for the long-wavelength pumps. A reasonable fit could not be obtained using a single exponential function. Note that these time constants represent the cumulative response of ampli-

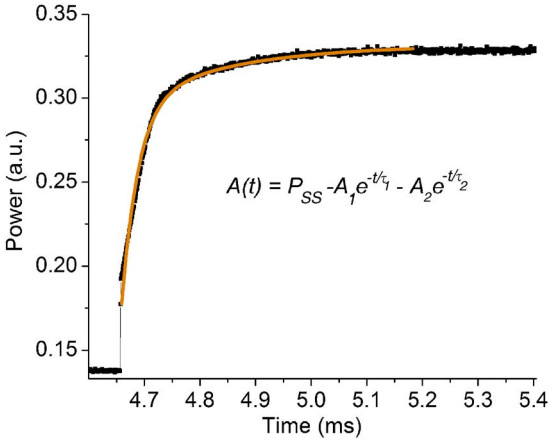


Fig. 3. Double exponential curve fit to the long-wavelength survivor response (1594 nm) at the input to the second span; P_{SS}: final power excursion; $A_{1,2}$: excursion amplitudes; $\tau_{1,2}$: 1/e time constants.

fiers reacting on similar time scales and the response is not expected to be purely exponential in particular due to pump–pump interactions [6].

Figure 4 provides two additional detailed views of the transient response for the long-wavelength survivor at the input to span 4 [Fig. 4(a)] and the short-wavelength survivor at the input to span 12 [Fig. 4(b)]. Each of the three basic amplifier responses is indicated, demonstrating that the very different time response can be viewed as a composite of the different amplifier responses adapting according to their respective saturation levels. The amplitude of the total surviving channel set power excursion is bounded by the size of the channel drop, assuming that the pump efficiency remains constant. The drop from 109 to 16 channels is 8.3 dB, however, due to ripple and tilt on the channels, the resulting total power change varied from 8–9 dB for the different cases. The initial channel-power excursion shown in Fig. 2 due to the loading amplifier is between 0.9 and 1.5 dB, depending on wavelength. This has the potential to grow to 8–9 dB. As the magnitude of the excursion grows within the first few spans, the time response will be a simple cumulative function contributed by each of the amplifiers. As the signal approaches the maximum excursion, the time response will adapt to the different maximum levels for each type of Raman interaction. In this light, the growth of an overshoot in Fig. 2 indicates that the maximum excursions for the copropagating Raman interactions are larger than for the counterpropagating Raman interactions. This effect will be caused by some combination of tilt, differences in the Raman pump efficiency for different channel sets, and ASE noise growth.

Thus the overshoot on the short-wavelength channel power is only observed as the excursions approach their maximum near the input to span 4. As the magnitude of the excursions varies with distance, the overshoot also varies, reaching a maximum near span 12 and then decreasing from span 12 to 18, so that it is no longer visible after span 18 as seen on the span 72 time trace. In contrast, EDFA-based systems with multistage amplifiers would exhibit an overshoot on all channels at the output of the first span that steepens with each span and persists to the end of the line [2]. Also note that the long-wavelength channels show a slight initial decrease (undershoot) in span 1 input power that is entirely due to the channel–channel interaction in the backward-pumped loading amplifier.

Further evidence that the overshoot is due to differences in the gain saturation levels for the different Raman interactions comes from the fact that the overshoots have very different rise and fall times. This effect is unlike overshoots observed on individual Raman amplifiers due to excess pump depletion, for which the rise and fall times of the overshoot are characteristic of the amplifier response time [6]. However, some overshoot and ripple that might be attributed to excess pump depletion is evident on several time traces. Figure 5 is a detailed view of the transient response at

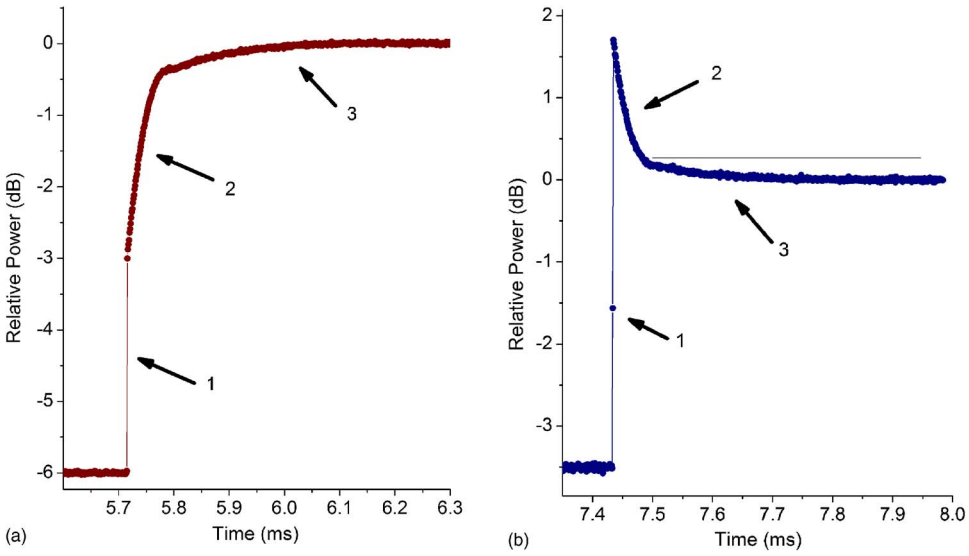


Fig. 4. Detailed views of the (a) long-wavelength surviving channel response and (b) short-wavelength surviving channel response. Three unique response features are evident: (1) copropagating Raman interactions; (2) backward-pumped discrete Raman amplifiers; and (3) backward-pumped distributed Raman amplifiers.

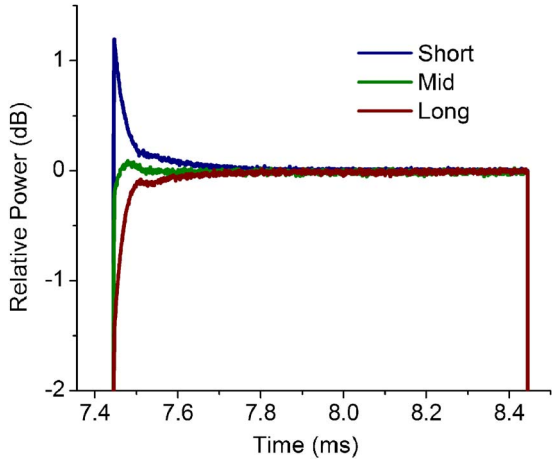


Fig. 5. Surviving channel transient response variation with wavelength at the loop output (tap M1).

the output of the loop (tap M1) following one round trip for short-, mid-, and long-wavelength survivors. The small ripple on the mid- and long-wavelength survivors occurs on time scales characteristic of the discrete Raman amplifiers and therefore may be influenced by excess pump depletion effects.

In summary, these results show that the Raman cascade transient response is a composite of the different time signatures of the various amplifier types used in the Raman system: distributed and discrete, with either copropagating or counterpropagating pumps. Initially, the power excursion exhibits a function that is characteristic of the cumulative power excursions from each amplifier. Based upon the time dependence of the response features, the maximum transient power excursion level is found to be dependent on the amplifier type and surviving channel wavelength. Once the maximum excursion levels are reached, the resulting response is formed by the relaxation between the different final excursion levels. Small features indicative of excess pump depletion were also observed. The magnitude of power excursion decreases over long distances, and this reduction is also amplifier and wavelength dependent.

4. Tilt Evolution: Long-Wavelength Survivors

To better understand the evolution of the different transient response functions, the power excursions were studied at the loop output as a function of distance over multiple recirculating loop round trips. Figure 6 shows the results comparing channels 1 (shortest wavelength, 1588 nm) and 16 (longest wavelength, 1594 nm) in the long-wavelength survivor set. Both channels exhibit a large increase in their respective power excursion from the loading response to the first round-trip output, which then

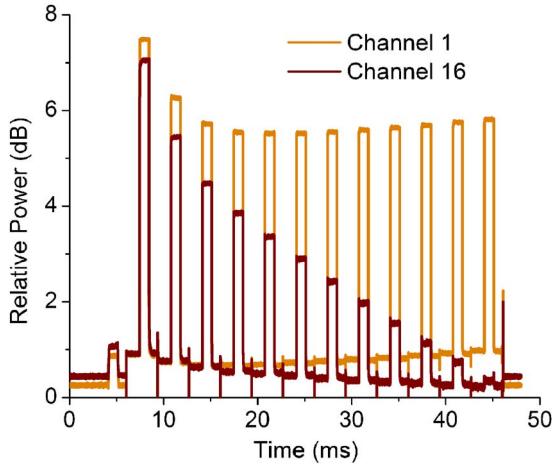


Fig. 6. Time evolution of the first [(a) 1588 nm] and last [(b) 1594 nm] channel in the long-wavelength surviving channel set.

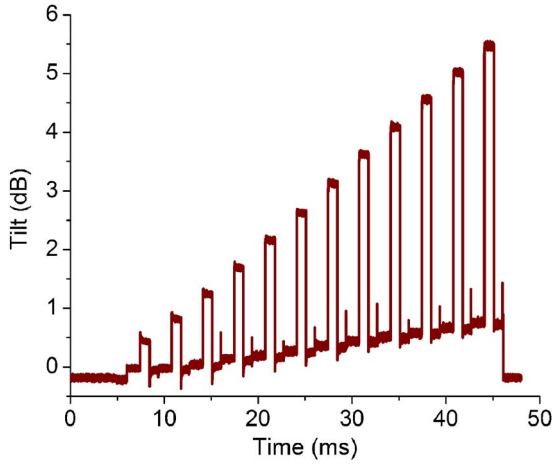


Fig. 7. Tilt between channels 1 and 16 in the long-wavelength survivor band as a function of loop round trips at the loop output (tap M1).

decays in subsequent round trips. After 1800 km, however, channel 1 levels off and increases slightly in power, whereas channel 16 continues to decrease. In Fig. 7, the difference between the two traces in Fig. 6 is plotted. A clear tilt is formed across the surviving channel band and grows linearly with distance. The common reduction in power among both channels up to 1800 km indicates that the mean excursion of the band is decreasing, whereas the leveling and rise of channel 1 at longer distances is due to a substantial slowing of the decay in the mean channel power.

Although the surviving channel band is small, the channel–channel Raman interaction would be expected to give a slight positive tilt with wavelength when all 109 channels are present. The loss of this tilt when the 93 shorter wavelength channels are dropped could be responsible for this steadily increasing tilt, assuming that the gain spectrum due to the Raman pumps remains constant. Since these longest wavelength channels are predominantly pumped by a strong long-wavelength pump in most amplifiers, the gain shape would not be expected to change substantially due to changes in the pump spectra.

The reduction in the mean power of the surviving channel group seen in Fig. 6 is found to correlate with the growth of ASE noise power at the location of the cut channels. In Fig. 8, the transient response at 1542 nm is plotted for the long-wavelength survivor set experiment, corresponding to the location of a cut channel. Over the first 1200 km, the ASE noise is observed to grow rapidly, completely replacing the original channel power. Some small additional growth occurs to 1800 km, before the ASE settles at a level 1–2 dB above the original channel power. Thus, the leveling off of the response of the first channel in the surviving channel band correlates with the ASE noise reaching a stable point filling in the lost channel power. The optical power spectra at 1800 km both before and after the transient event are shown in Fig. 9. The ASE noise over much of the short-wavelength end of the spectrum has replaced the

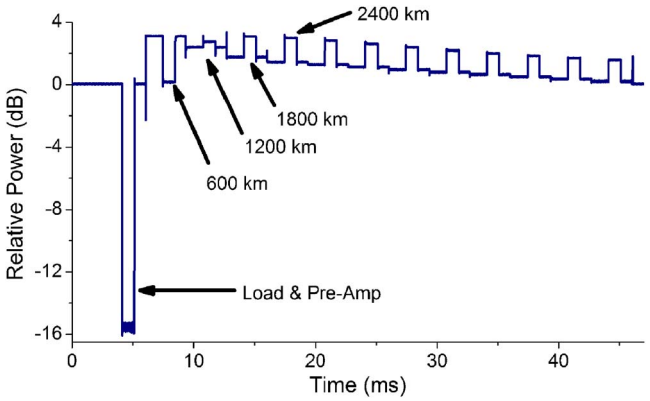


Fig. 8. Transient response at 1548 nm, corresponding to the cut channels for the long-wavelength survivor set.

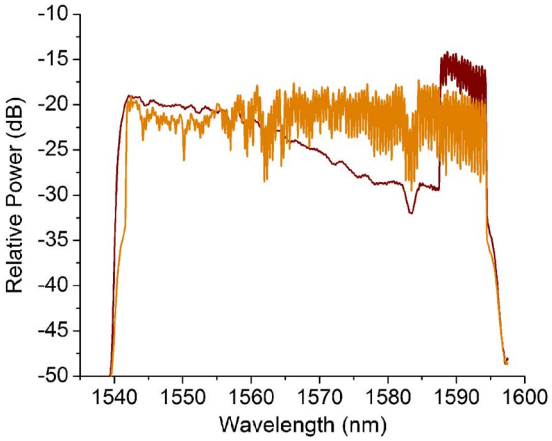


Fig. 9. Optical power spectra for the long-wavelength survivor case before (gold) and after (red) the transient event, recorded at 1800 km at the loop output.

lost channels at those wavelengths. Near to the surviving channel band, the ASE noise has remained at a low level characteristic of the usual OSNR degradation during propagation. The surviving channels appear to have sufficiently saturated the longest-wavelength pumps to inhibit excess ASE growth. However, the short-wavelength pumps do not appear to be substantially depleted by the long-wavelength pumps and therefore provide excess gain at short wavelengths. Indeed, one would expect as the power in the surviving channels approaches the power of the full 109 channels (+8.3 dB excursion), that the long-wavelength pumps would be excessively depleted, leaving the short-wavelength pumps to funnel additional gain to ASE growth.

5. Tilt Evolution: Short-Wavelength Survivors

A similar analysis was conducted for the surviving channels in the short-wavelength surviving channel band experiment. The transient response over multiple round trips at the loop output is shown for channels 1 and 16 of the short-wavelength set in Fig. 10. Again both channels exhibit large power excursion growth over the first round trip and then decay in subsequent round trips. However, channel 1 shows a marked increase in power excursion beyond 1800–2400 km. For channel 16, the power excursion drops ~–1.5 dB per loop round trip (600 km) from 600 to 1800 km and then slows to ~–0.2 dB per round trip beyond 1800 km. This behavior again indicates a reduction in the total surviving channel set power excursion for distances up to 1800 km that levels off at longer distances. The tilt within the surviving channel set, however, continues to grow beyond 1800 km.

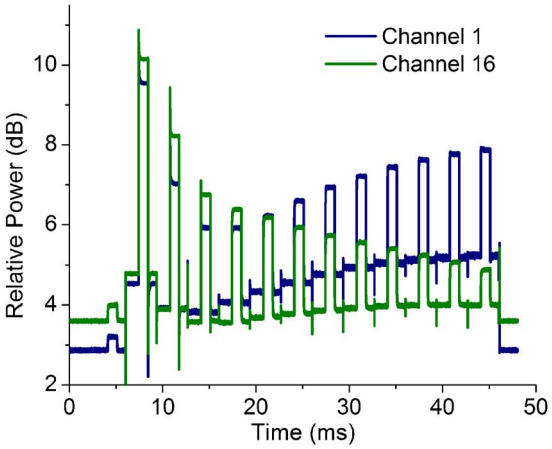


Fig. 10. Transient response of channels 1 and 16 of the short-wavelength surviving channel set at the loop output over multiple round trips.

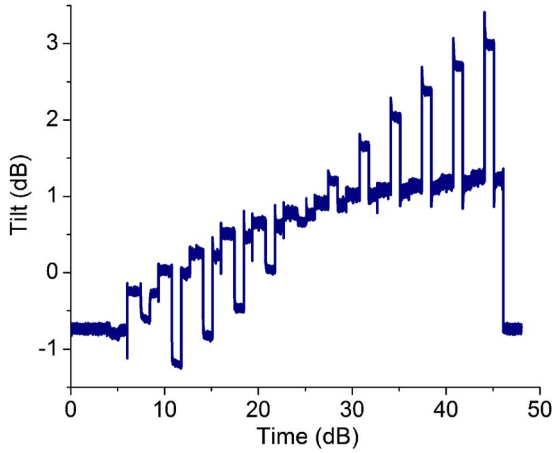


Fig. 11. Tilt between channels 1 and 16 in the short-wavelength surviving channel set at the loop output for multiple loop round trips.

In this case, the tilt between channels 1 and 16 (Fig. 11) differs in that it undergoes a sign reversal, first increasing negative to 1200 km and then tilting back toward positive steadily over the remaining distance, changing sign near 3600 km. The tilt also demonstrates an overshoot that grows with distance. Based upon the time response of the overshoot (as described above), the tilt appears to grow more rapidly in the forward-pumped amplifiers.

For the short-wavelength survivor case, the ASE noise was again found to rapidly fill in at the cut channel wavelength region farthest from the surviving channel band. The time dependence of the cut channel at 1591 nm measured at the loop output (M1 tap) is shown in Fig. 12. The noise power is within 3 dB of the original channel power after two round trips. Note, however, that the ASE power exhibits a strong undershoot during the first three round trips. This effect provides insight into the overshoots observed on the surviving channel power response at short wavelengths. The ASE noise power grows more slowly with distance on the time scale of the copropagating Raman interactions. Therefore, the maximum power excursion available to the surviving channels will be larger within the copropagating Raman interaction time window (100 ns), leading to the overshoots observed in Fig. 2. This indicates that the short-wavelength surviving channels are more effective at depleting the copropagating Raman pumps, reducing the growth of ASE noise even at long wavelengths. Differences in the gain saturation between copropagating and counterpropagating Raman amplifiers and the channel–channel Raman interaction can contribute to the different pump depletion.

In Fig. 13, the total power (recorded by removing the OTF at the loop output) is observed to recover by 1800 km and even slightly increase at longer distances, due to more efficient pump conversion to the signal band. Note that similar to Fig. 2, the

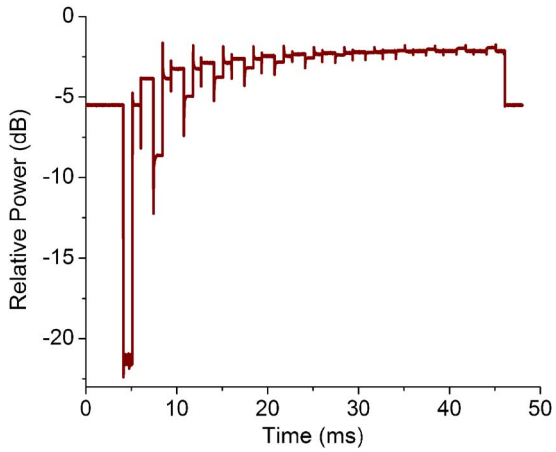


Fig. 12. Transient response at 1591 nm, corresponding to the cut channels for the long-wavelength survivor set.

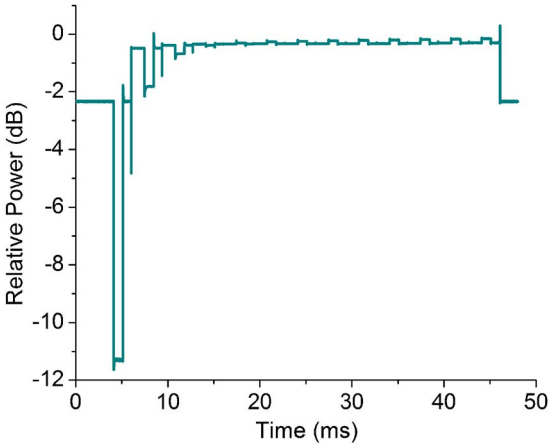


Fig. 13. Total power at the loop output for the short-wavelength surviving channel set experiment.

maximum excursion of the surviving channels does not reach the 8–9 dB required to fully recover the total power after one round trip. This effect is expected because the broadband pumps will be less efficient when pumping a small band of channels compared to channels distributed over the full band. Thus, the growth of ASE noise may be required in order to completely recover the total power. The surviving channel power excursion magnitude and tilt correlates with the growth of the ASE noise and recovery of the total power. In this case, however, the tilt evolution changes sign and cannot be accounted for by the lost channel–channel interaction. The short-wavelength surviving channels in fact obtain strong contributions from several different pumps and one would expect that the ripple and tilt would depend on the relative amplitude of these different pumps. As the ASE noise loads the long-wavelength pumps, this will impact the relative pump depletion of the short-wavelength pumps. The short-wavelength channels may also lose power to the ASE noise through Raman pumping. However, if the tilt were due to this effect then one would expect that the shortest-wavelength channel would be the most heavily depleted and therefore should result in a positive tilt with wavelength, which is opposite to what is observed. The fact that the surviving channel set tilt grows differently on the copropagating and counterpropagating pump amplifiers indicates that the channel–channel interaction may be assisting the tilt similar to the tilting in Fig. 7.

6. Conclusion

The propagation of fast power transients was measured in a broadband all-Raman amplified transmission system for three different surviving channel configurations. Different time signatures were shown to develop due to differing levels of gain saturation and channel–channel Raman coupling between the forward- and backward-pumped distributed amplifiers and the backward-pumped discrete amplifiers. Unlike EDFA-based systems, transient effects in Raman amplified systems take multiple spans to reach a maximum and damp at longer distances due to the growth of ASE noise that occurs in uncontrolled transient events. Likewise, changes in the magnitude and tilt of the channel power excursions coincide with the growth of ASE noise replacing the cut channels, at distances greater than 1200 km in these experiments. The time signatures were shown to not only evolve due to excess pump depletion, but more strongly in a manner attributable to different maximum power excursions within the various amplifiers. The growth of ASE noise was also shown to vary among the amplifier types, and the different growth rates again correlated with features in the channel power transient time signatures. The evolution of the channel power tilt could not be accounted for by changes in the channel–channel interactions alone and therefore must include contributions from ripple and tilt formed through varying pump interactions.

References and Links

1. L. F. Mollenauer, A. R. Grant, X. Liu, X. Wei, C. Xie, I. Kang, and C. Doerr, “Demonstration

of 109 × 10 G dense WDM over more than 18000 km using novel, periodic-group-delay-complemented dispersion compensation and dispersion-managed solitons," in *European Conference on Optical Communications (ECOC 2003)* (Institution of Electrical Engineers, 2003), postdeadline paper Th4.3.4.

2. Y. Sun, A. K. Srivastava, J. L. Zyskind, J. W. Sulhoff, C. Wolf, and R. W. Tkach, "Fast power transients in WDM optical networks with cascaded EDFAs," Electron. Lett. **33**, 313–314 (1997).
3. C. Tian and S. Kinoshita, "Analysis and control of transient dynamics of EDFA pumped by 1480- and 980-nm lasers," J. Lightwave Technol. **21**, 1728–1734 (2003).
4. G. Luo, J. L. Zyskind, J. A. Nagel, and M. A. Ali, "Experimental and theoretical analysis of relaxation-oscillations and spectral hole burning effects in all-optical gain-clamped EDFA's for WDM networks," J. Lightwave Technol. **16**, 527–533 (1998).
5. C.-J. Chen and W. S. Wong, "Transient effects in saturated Raman amplifiers," Electron. Lett. **37**, 371–372 (2001).
6. M. Karasek and M. Menif, "Channel addition/removal response in Raman fiber amplifiers: modeling and experimentation," J. Lightwave Technol. **20**, 1680–1687 (2002).
7. E. Schulze, M. Malach, and F. Raub, "All-Raman amplified links in comparison to EDFA links in case of switched traffic," in *European Conference on Optical Communications (ECOC 2002)* (IEEE, 2002), paper symposium 3.08.
8. S. Gray, "Transient gain dynamics in wide bandwidth discrete Raman amplifiers," in *Optical Fiber Communications Conference (OFC 2002)* (Optical Society of America, 2002), paper ThR2.
9. A. Bononi and M. Papararo, "Transient gain dynamics in saturated counter-pumped Raman amplifiers," in *Optical Fiber Communications Conference (OFC 2002)* (Optical Society of America, 2002), paper ThR1.
10. A. R. Grant and D. C. Kilper, "Signal transient propagation in an all Raman amplified system," in *Optical Fiber Communications Conference (OFC 2004)* (Optical Society of America, 2004), paper ThT3.